HHS Public Access

Author manuscript

Acta Biomater. Author manuscript; available in PMC 2019 December 01.

Published in final edited form as:

Acta Biomater. 2018 December ; 82: 158–170. doi:10.1016/j.actbio.2018.10.027.

Pharmacokinetics and efficacy of orally administered polymeric chloroquine as macromolecular drug in the treatment of inflammatory bowel disease

Shrey Kanvinde[1], **Yashpal Singh Chhonker**[2], **Rizwan Ahmad**[4], **Fei Yu**[1], **Richard Sleightholm**[1], **Weimin Tang**[1], **Lee Jaramillo**[1], **Yi Chen**[1], **Yuri Sheinin**[¶,3], **Jing Li**[1], **Daryl J. Murry**[2], **Amar B Singh**[4], and **David Oupický**[1,*]

[1]Center for Drug Delivery and Nanomedicine, Department of Pharmaceutical Sciences, University of Nebraska Medical Center, Omaha, NE 68198

[2]Department of Pharmacy Practice, University of Nebraska Medical Center

[3]Department of Pathology and Microbiology, University of Nebraska Medical Center, Omaha, Nebraska, United States University of Nebraska Medical Center

[4]Department of Biochemistry and Molecular Biology, University of Nebraska Medical Center

Abstract

Inflammatory bowel disease is a chronic inflammation of the gastrointestinal tract with poor understanding of its pathogenesis and no effective cure. The goal of this study was to evaluate the feasibility of orally administered non-degradable polymeric chloroquine (pCQ) to locally reduce colon inflammation. The pCQ was synthesized by radical copolymerization of N-(2-hydroxypropyl)methacrylamide with methacryloylated hydroxychloroquine (HCQ). The anti-inflammatory activity of orally administered pCQ versus HCQ was tested in a mouse model of colitis induced by *Citrobacter rodentium (C. rodentium)*. Single-dose pharmacokinetic and biodistribution studies performed in the colitis model indicated negligible systemic absorption ($p \leq 0.001$) and localization of pCQ in the gastrointestinal tract. A multi-dose therapeutic study demonstrated that the localized pCQ treatment resulted in significant reduction in the colon inflammation ($p \leq 0.05$). Enhanced suppression of pro-inflammatory cytokines IL-6 ($p \leq 0.01$) and IL1-β and opposing upregulation of IL-2 ($p \leq 0.05$) recently reported to be involved in downstream anti-inflammatory events suggested that the anti-inflammatory effects of the pCQ are mediated by altering mucosal immune homeostasis. Overall, the reported findings demonstrate a potential of pCQ as a novel polymer therapeutic option in inflammatory bowel disease with the potential of local effects and minimized systemic toxicity.

Abstract

[*]Corresponding author. david.oupicky@unmc.edu.

[¶]present address: Department of Laboratory Medicine and Pathology, University of Minnesota

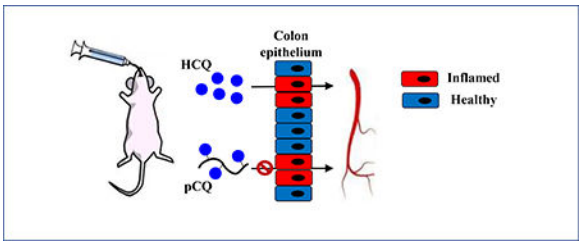

Keywords

Inflammatory bowel disease; colitis; *Citrobacter rodentium*; chloroquine; oral administration; polymeric drug; pharmacokinetics

1. INTRODUCTION

Inflammatory bowel disease (IBD) is a chronic remittent inflammatory condition of the gastrointestinal (GI) tract that manifests itself in two major forms – ulcerative colitis (UC) and Crohn's disease (CD) [1]. UC involves continuous inflammation, usually in the colon and rectum, while CD involves patchy inflammation, which can be present anywhere in the GI tract. Despite intensive research, IBD has a poorly understood pathogenesis and no effective cure. Conventional palliative therapies, which include anti-inflammatory and immunosuppressive agents represent major treatment options that can temporarily induce and maintain remission but carry significant side-effects [2]. Moreover, despite these available treatment options, 70% of IBD patients require at least one surgical intervention in their lifetime [3].

Activation of the immune cells and production of pro-inflammatory cytokines like TNFα, IL-6, IFNγ, and IL-1β are some of the hallmarks of IBD [4]. Inhibition of the pro-inflammatory cytokines represents a promising avenue in IBD therapy. As a result, the current mainstay of IBD therapy relies on orally administered small molecule anti-inflammatory drugs and systemically given biologics [5]. Due to the chronic nature of IBD, patients remain on various treatments for life and thus long-term effects of the therapy represent a significant concern. Aminosalicylates are a first-line therapy for induction and maintenance of remission for mild and moderate IBD [6]. Aminosalicylates have high systemic absorption, high rates of intolerance, and their long term use may cause multiple side effects including nausea, vomiting, pancreatitis and systemic lupus erythematosus [7]. Corticosteroids are used for induction of remission in moderate and severe IBD, but they provide limited benefits for maintenance or healing mucosal lesions. Long term use of corticosteroids has been implicated in musculoskeletal diseases, metabolic abnormalities, blood pressure changes and immunosuppression [8]. Biologics are a relatively new class of drugs used to induce remission in steroid-refractory disease or to maintain remission in patients for whom aminosalicylates provide inadequate relief. The bulk of this class is represented by systemically administered anti-TNFα antibodies (e.g. Infliximab) and although effective, such broad systemic anti-inflammatory treatment faces serious limitations due to systemic immune suppression, which renders patients susceptible to opportunistic infections and exposes them to a greater risk of cancer [9]. Considering the

side effects that arise due to the systemic IBD treatments, oral administration is a preferred route as it can give access to inflammation specifically localized in the colon [10, 11].

The main challenge in the development of oral IBD therapies are the physiological changes in the course of the disease [11]. The GI environment is diverse and factors like residence time, changes in pH, enzymatic or microbial degradation play an important role in drug delivery. These factors vary significantly between IBD patients and healthy individuals. For example, colonic transit time ranges from 6 to 70 h in IBD patients as compared to 4 to 6 h in healthy individuals [12, 13]. Colon pH in IBD patients is significantly lower than in healthy colon [14, 15]. The epithelial barrier represents one of the tightest barriers in the human body [16]. It consists of tight junction proteins, which selectively regulate the transport across the colonic epithelium. Inflammation alters the permeability of this barrier and consequently, the protective mechanisms significantly alter the physiology of the colonic epithelium, which in turn affects drug transport.

Many strategies have been explored for local oral drug delivery to the inflamed colon. Conventional delivery systems are designed to function well in healthy intestinal pH but may perform poorly in IBD [11, 17]. Nanoparticles and microparticles have been researched with respect to their size as well as charge for accumulation in inflamed colon. Results have shown that passively targeted systems with particle size ranging from 100 to 300 nm and positive surface charge preferentially accumulate in the inflamed colon [18, 19]. The specificity of these systems can be enhanced by incorporation of targeting ligands (e.g. lectins, mannose) that bind receptors overexpressed in the inflamed colon [20, 21]. Conjugating small molecule drugs to polymers has been explored as another delivery strategy to enhance colon retention [22]. Dexamethasone-poly(dimethylamino)ethyl methacrylate conjugates and dextran-budesonide conjugates have been reported as potential orally administered alternatives to free dexamethasone and budesonide that overcome systemic side effects and pH lability, respectively [23, 24]. Although intended to treat local inflammation, most of the polymer-drug conjugates have been synthesized with a goal of releasing free drug in the colonic environment. As a result, the released drug is still absorbed systemically.

Chloroquine (CQ) is commonly used to prevent and treat malaria caused by *Plasmodium (P) vivax*, *P. ovale*, and *P. malariae*. In recent years, CQ has also found growing anti-inflammatory application in the treatment of autoimmune disorders like rheumatoid arthritis and lupus erythematosus [25]. Despite its decades-old use, the exact anti-inflammatory mechanism of CQ is unknown. Various reports attempted to elucidate the mechanism of action by studying the effect of CQ on T-cell activation and T-cell mediated immune response [26, 27]. In murine model of IBD, CQ showed its anti-inflammatory effect via inhibition of toll-like receptor signaling pathway resulting in a reduction of T cell proliferation and cytokine production, indicating the promise of CQ in treating IBD [28]. However, it has been clinically proven that long-term use of CQ can result in severe ocular side effects including blurred vision and retinopathy [29, 30]. We have synthesized a polymeric form of CQ (pCQ) [31] and used it here as a non-degradable polymeric form of the drug with the goal of minimizing systemic exposure and thus circumventing safety limitations of CQ in IBD. We hypothesized that due to its macromolecular character, oral

administration of pCQ will prevent systemic absorption and restrict the anti-inflammatory effect to the colon as a new strategy to enhance local anti-inflammatory therapies of IBD. In the current study, oral pharmacokinetics and evaluated therapeutic efficacy of pCQ were analyzed using a widely used mouse model of IBD induced by oral administration of *C. rodentium*.

2. MATERIALS AND METHODS

2.1 Materials.

Hydroxychloroquine (HCQ) sulfate (98 %), triethylamine, Deuterated dimethyl sulfoxide (DMSO-d6) (99.8 %) and deuterated chloroform-d (99.8 %) were obtained from Acros Organics (Fisher Scientific). Methanol, acetonitrile were purchased from Fisher Scientific. pCQ (Fig. 1) with 16.7 mol % of CQ and weight average molecular weight 60 kDa was synthesized and characterized as previously reported [31].

2.2 *C. rodentium* model of colitis.—Male C57BL/6 mice (6 weeks old, 18–20 g) were obtained from Charles River Laboratories and used for all *in vivo* studies. Prior to the start of the study, the animals were acclimatized for one week and given *ad libitum* access to food and water. All animal experiments were conducted according to the protocol 13–358-09-FC approved by the University of Nebraska Medical Center Institutional Animal Care and Use Committee. *C. rodentium* was used to induce colitis in mice as previously described [32]. Bacterial glycerol stock was streaked onto Luria broth (LB) agar plates and the bacterial colonies were grown overnight at 37 °C. A single colony was inoculated into 5 mL of 2 % LB broth and incubated at 37 °C, 280 rpm overnight to obtain a saturated primary culture. On the day of the experiment (Day 0), 2 mL of the primary culture was added into 300 mL of LB and the inoculum was placed on a shaker at 37 °C at 280 rpm for 6 h. Bacterial optical density was measured at 600 nm. Bacteria were diluted with LB and delivered to mice (n=15) via oral gavage in a 100 μL volume containing 5×10^8 colony forming units (CFU). Healthy control group (n=5) was orally administered 100 μL of LB.

2.2.1 Cytokine analysis.—Five mice were sacrificed at each time-point (day 1, 10 and 14 after oral gavage of the *C. rodentium*) using carbon dioxide combined with cervical dislocation. The colons were excised, cleaned, and their weight and length recorded. The entire colon was frozen and stored at −80 °C. The colon was homogenized in 1.5 mL radioimmunoprecipitation assay (RIPA) buffer using TissueLyserII (Qiagen) and the homogenates centrifuged at 15,000 × g for 15 min at 4 °C. The supernatant was analyzed for cytokine levels using ProcartaPlex™ Multiplex Immmunoassay (Invitrogen) following the manufacturer's protocol. Briefly, magnetic beads coated with different cytokine antibodies were added at the required dilution to 96-well plate. Supernatants from the tissue homogenates and supplied fluorescent standards were added to the respective wells. The cytokines were measured by adding a detection antibody followed by addition of Streptavidin-PE. The beads were read on Luminex™ LX 200 Analyzer. The data obtained were analyzed using ProcartaPlex™ Analyst software to obtain cytokine concentrations.

2.3 Pharmacokinetics and biodistribution.

The pharmacokinetics and biodistribution of single dose pCQ were evaluated in a mouse model of IBD. Colitis was induced as described above and on day 14, the mice were given single dose of HCQ (30 mg/kg) or pCQ (equivalent to 30 mg/kg HCQ) in 200 μL of deionized water via oral gavage. Both HCQ and pCQ were fully soluble at the tested concentrations. Blood was collected from the submandibular vein at 0.5, 1, 2, 4, 8, and 24 h post-administration. The animals were sacrificed, and organs harvested at 0.5, 2, 8, and 24 h post-administration and stored at −80 °C until further use. The mice were randomized to selected sampling times so that three blood samples and one terminal tissue collection were obtained from each.

Blood and tissue samples were processed by two methods to determine free HCQ and total HCQ. For the first method, HCQ was isolated by a simple extraction as previously described [33]. The second method utilized base hydrolysis to release HCQ covalently bound to pCQ and subsequent HCQ extraction using solid phase extraction (SPE). Tissues were homogenized in water prior to loading to the SPE cartridge. The calibration and quality control samples were separately prepared for HCQ and pCQ by spiking 10 μL of appropriate calibration stock of HCQ and pCQ, in 100 μL of blank biomatrix, and 10 μL of internal standard solution (1.0 μg/mL) added. For the study, 25 μL of blood and 100 μL of tissue homogenate were used. 400 μL of 1 M NaOH, 600 μL water and 100 μL methanol were added and the samples were incubated at 50 ºC for 1 h to hydrolyze HCQ from the pCQ. Subsequently, 400 μL 2 % formic acid was added and the samples were vortexed for 30 s and centrifuged at 1301 x *g* for 10 min. The SPE was carried out using Oasis HLB 3cc, 60 mg extraction Cartridge (Waters, Inc). Cartridges were pre-conditioned with 1 mL acetonitrile followed by 1 mL water. Samples were loaded to the cartridges and washed with 2 mL of aqueous 15 % methanol and dried at high vacuum for 15 min. Analytes were eluted with 2 mL of acetonitrile. The eluents were collected in glass tubes and dried under nitrogen in water bath at 50 °C. The dry residues were reconstituted in 400 μL 0.1 % formic acid: methanol mixture (60:40) and centrifuged at 13000 x g and 10 μL supernatant was injected into the HPLC. The LC-MS/MS conditions were as previously described [33]. The assay was linear over the range of 1 to 2000 ng/mL.

The pharmacokinetic parameters of HCQ and pCQ in blood and tissues were calculated using non-compartmental analysis with Phoenix WinNonlin 6.3 (Pharsight Corporation). The area under the curve ($AUC_{0-\infty}$) was estimated using the linear trapezoidal method from 0-t_{last} and extrapolation from t_{last} to infinity based on the observed concentration at the last time point divided by the terminal elimination rate constant (λ). The elimination half-life ($t_{1/2}$) was calculated as 0.693/k. Apparent clearance (Cl/F) and the apparent volume of distribution of the elimination phase (V_d/F) were calculated as dose/$AUC_{0-\infty}$ and dose/k*$AUC_{0-\infty}$, respectively. The mean residence time (MRT) was calculated as $AUMC_{0-\infty}$/$AUC_{0-\infty}$. Mean tissue concentrations were calculated and expressed as ng/g tissue. The absolute bioavailability was calculated as: $F_{abs} = \frac{AUC_{po} \times D_{iv}}{AUC_{iv} \times D_{po}}$; where AUC_{po} and AUC_{iv} are the areas under the curve after oral (po) and i.v. administration and D_{iv} and D_{po} are the corresponding doses.

2.4 Therapeutic efficacy.

Colitis was induced as stated above and mice were randomly assigned to healthy, HCQ, and pCQ treatment groups (n=5) and untreated group (n=8). The group size of 5 was selected based on a pilot study and power analysis. Starting day 1, the mice received oral gavage of either HCQ or pCQ every other day (30 mg/kg HCQ equivalent in 200 μL sterile deionized water). Untreated and healthy controls were administered 200 μL sterile deionized water. On day 14, the mice were sacrificed, and the colons were harvested. The colon was opened longitudinally, cleaned of fecal matter, and excised into two parts along the length, which were stored accordingly for determination of cytokine mRNA levels by real time polymerase chain reaction (RT-PCR) and histological analysis.

2.4.1 RT-PCR.—Colon samples from the therapeutic study were stored in RNAlater™ (Thermo Fisher Scientific Inc.) at 4 °C for 48 h to allow sufficient time for tissue penetration followed by removal of excess solution. The tissues were then stored at −80 °C until further processing. Stored frozen tissues were homogenized in TRIzol™ (Thermo Fisher Scientific Inc.) reagent using TissueLyser II (Qiagen) and mRNA was isolated from the homogenized tissues according to manufacturer's protocol. The extracted mRNA was quantified using Nanodrop One^{c} UV-Vis spectrophotometer (Thermo Fisher Scientific Inc.). The cDNA was synthesized from the mRNA using High-Capacity cDNA Reverse Transcription Kit with RNase Inhibitor per the manufacturer's protocol (Thermo Fisher Scientific Inc.). A volume corresponding to 1 μg of RNA as determined by UV spectrometer was used for cDNA synthesis. Synthesized cDNA was stored at −20 °C until further use. RT-PCR was carried out using the synthesized cDNA from colon tissue samples to determine the levels of mRNA of the target genes. Healthy and untreated colons were used as controls. cDNA was mixed with 0.2 μM of primer pair of gene of interest (Table 1) and iTaq™ Universal SYBR® Green Supermix (Biorad) into an optical reaction tube (Qiagen). The RT-PCR reaction was carried out in Rotor-Gene Q 2plex thermal cycler (Qiagen) using the following cycle program: 95 °C for 3 minutes; 40 cycles 60 °C for 30 seconds. Results obtained from the RT-PCR were analyzed by Livak's Ct method to determine the fold change in gene expression.

2.4.2 Histological evaluation.—The longitudinally opened colons were rolled into a Swiss roll from distal to proximal end. The rolls were fixed for 24 h in 4 % paraformaldehyde, embedded in paraffin, sectioned and stained with hematoxylin and eosin (H&E). The stained sections were evaluated by a pathologist without the knowledge of the identity of the samples using a light microscope. Histopathological scores were assigned based on criteria as previously described [34]. Scoring was performed based on severity of epithelial injury (graded 0–3, from absent to mild including superficial epithelial injury, moderate including focal erosions, and severe including multifocal erosions), the extent of inflammatory cell infiltrate (graded 0–3, from absent to transmural), and goblet cell depletion (0–1). For each tissue, a numerical score was assigned in a blinded manner to prevent bias. Scores from each tissue section group were averaged to obtain a mean histopathological score. Crypt heights were measured using ImageJ software, with 10 measurements taken in distal colons (lower one-third of the entire colon) of each mouse. Only well-oriented and intact crypts were measured. Tissue sections were stained for cleaved caspase 3 (CC3), macrophage infiltration (CD68) and STAT3. CC3 positive cells in

the entire colon roll were counted at 20x magnification. Results were expressed as mean CC3 positive cells per entire colon roll. CD68 positive cells were counted in five randomly chosen areas in the distal colon. *C. rodentium* affects the distal colon more than the proximal colon and we have thus selected areas in the lower third of the colon rolled as a swiss roll (distal to proximal direction). The five areas selected were top, bottom, left, right and center and the same areas were counted for all the colon samples from different treatment groups. As a result, the areas in which the CD68 positive cells were counted were matched at high power field (HPF) to ensure that the selected areas were reasonably matched for location. Results were expressed as mean of CD68 positive cells per HPF. For quantitation of STAT3 expression, four random images were taken from each section and cells with positive nuclear STAT3 staining were counted with number of crypts in each image. Results of nuclear STAT3 were expressed as fold change in nuclear STAT3 positive cells/crypt/field compared to healthy control.

2.5. Statistics.

Mann-Whitney test was used for statistical analysis of mean differences between treatment groups for biodistribution studies. One-way ANOVA followed by Tukey multiple comparison test was used for statistical analysis of mean differences among multiple groups. A value of $p < 0.05$ was considered statistically significant. All statistical analysis was performed using Graphpad Prism v5 (ns = not significant, * = $p \leq 0.05$, ** = $p \leq 0.01$, *** = $p \leq 0.001$).

3. RESULTS AND DISCUSSION

The main hypothesis of this study was that the non-degradable and macromolecular nature of pCQ will significantly restrict oral bioavailability of HCQ and thus allow us to test how local colon effects contribute to the overall anti-inflammatory activity of HCQ. Based on previous studies, it was hypothesized that pCQ will act as a polymeric drug with pronounced ability to inhibit inflammatory cell infiltration in the colon. The synthesis of pCQ by copolymerization of N-(2-hydroxypropyl)methacrylamide (HPMA) with methacryloylated HCQ has been previously reported (Fig. 1) [31]. Our previous studies found that pCQ had lower cytotoxicity than the parent small molecule HCQ [31]. For example, we found that while the IC_{50} of HCQ in HepG2 cells was 42 μg/mL, pCQ had an estimated IC_{50} >2,000 μg/mL.

3.1 *C. rodentium* mouse model of colitis

One of the major challenges in testing novel oral drug delivery systems in IBD is mimicking the complexities of the GI environment *in vitro*, particularly because of the diversity in the pH as well as presence of various enzymes [15]. Consequently, animal models form an indispensable part of the IBD research [35]. Colitis induced by *C. rodentium* is frequently used for modelling IBD in mice [34, 36–43]. *C. rodentium* is murine-specific bacteria that is closely related to important human pathogen *E. coli*. It attaches to the apical side of the colon epithelium and invades the colon wall, thus eliciting an immune response [32]. In addition to being well characterized for understanding host responses to enteric bacteria, it produces robust colitis characterized by elongation of crypts, immune cell infiltration, and

goblet cell depletion. This model was selected for the present studies over chemical injury models like DSS-induced colitis because of recent reports that have challenged the biorelevance of the DSS model from a pathological perspective [44]. Furthermore, DSS forms nanosized vesicles with fatty acids in the colon and is deposited onto the colonic epithelium, essentially forming a physical barrier, which can potentially interfere in the interaction between polymeric drug delivery systems and the intestinal tissue [45]. In addition, interference of DSS with RT-PCR is an established concern [46].

Initially, a study was conducted to confirm that the *C. rodentium* model exhibited expected pathobiology similar to the human IBD. As expected, an upregulation in the expression of pro-inflammatory cytokines was observed over 14 days after single oral dose of the bacteria (Fig. 2a). IL-6 was the most upregulated cytokine with almost 30-times higher peak levels than healthy controls. Other pro-inflammatory cytokines showed a similar trend. Further, the colons from mice infected with the bacteria showed significant reduction in length (Fig. 2b) and a contrasting increase in weight (Fig. 2c) as a result of the inflammation and edema. Histologically, colons of the infected mice exhibited inflammation-associated epithelial changes evidenced by crypt elongation, crypt fall-out, presence of apoptotic cells, and significant inflammatory cell infiltration. Distal colon showed more pronounced changes than the proximal colon, which was consistent with previous findings suggesting that *C. rodentium* preferentially colonizes the distal colon [47]. Although no single mouse model captures the complexity of the human IBD pathophysiology, the observed parameters correlate well with the chronic inflammatory changes, which occur during the development of human IBD. Overall, these findings supported the suitability of this animal model for the proposed study.

3.2 Pharmacokinetic study

3.2.1 Blood Pharmacokinetics—pCQ contains HCQ attached by a potentially hydrolyzable ester linker and it was thus important to distinguish between polymer-conjugated HCQ and free HCQ released from pCQ to make sure it was not getting hydrolyzed *in vivo* (Fig. 1). This goal was achieved by using two LC-MS/MS analytical methods. First, HCQ was quantified using a simple extraction from blood and tissues to determine the amount of HCQ that was released from pCQ by hydrolysis in the GI tract, blood, or liver. In the second method, an alkaline hydrolysis step that was optimized to fully hydrolyze the ester linker between HCQ and the polymer was included, thus providing information on the total (polymer bound + hydrolyzed) HCQ. The difference in the HCQ amount obtained from the two methods was used to calculate the percent of HCQ in the tissues that remained bound to the polymer. The HCQ amount quantified by both methods was similar in blood and tissues in animals treated with HCQ.

The blood concentration vs. time profile for the HCQ and pCQ after oral administration is shown in Fig. 3. The pharmacokinetic parameters of pCQ were determined from the total HCQ content in the blood and thus represent a combined pharmacokinetics of polymer-bound and hydrolyzed HCQ (Table 2). The drug reached a maximum concentration in blood (C_{max}) of 2,342.6 ± 46.3 (HCQ) and 12.2 ± 1.7 ng/mL (pCQ). The values of area under curve ($AUC_{0-\infty}$) were determined as 28,182.4 ± 1,475.8 and 231.3 ± 48.8 h×ng/mL for

HCQ and pCQ treatment, respectively. In comparison to HCQ, the pCQ exhibited a significant reduction of C_{max} (~192-fold) and $AUC_{0-\infty}$ (~122 fold) indicating that conjugation of HCQ to the polymer dramatically reduced its absorption. The absolute bioavailability (oral-to-i.v.), was 0.4 % for pCQ compared to 80 % for HCQ, indicating that the pCQ substantially reduced HCQ bioavailability and was retained in the GI tract. One pharmacokinetic disadvantage of HCQ and its metabolites is their exceptionally long residence time in the blood that contributes to the undesired side effects of chronic CQ treatments. In the pCQ treatment group, HCQ levels were substantially lower in the systemic circulation, suggesting that prolonged exposure to HCQ and metabolites will not be a major systemic toxicant. This is an important finding for a small molecule drug like HCQ which has high systemic bioavailability resulting in high non-specific tissue exposure. Reduction in systemic absorption and bioavailability is important for local therapy and reduction of systemic toxicities and the developed pCQ resulted in very different blood pharmacokinetic profile compared to HCQ.

3.2.2 Colon and liver distribution

There have been numerous reports indicating that conjugating small molecule drugs to polymers can change their pharmacokinetics and pre-dispose them to preferential accumulation in specific tissues. The effect of differences in blood pharmacokinetics on relative distribution of pCQ and HCQ to the colon and liver following oral administration was assessed in the *C. rodentium* colitis.

The colon and liver pharmacokinetics and distribution results are shown in Table 3 and Fig. 4. HCQ and pCQ reached a C_{max} in colon of 10,304 ± 746 and 7,121 ± 2,984 ng/mL, respectively. The colon $AUC_{0-\infty}$ was 208,917 ± 55,806 for HCQ and 94,515 ± 35,363 h×ng/mL for pCQ treatment. HCQ appeared to show higher colon concentrations than pCQ probably due to faster transit time, but the difference did not reach statistical significance. Both HCQ and pCQ showed increasing accumulation in the colon from the time of administration until at least 8 h, with subsequent decline by 24 h (Fig. 4). Both pCQ and HCQ showed similar colon pharmacokinetic behavior. The T_{max} for HCQ and pCQ occurred at 8 h. However, major differences were observed in the hepatic pharmacokinetic parameters of pCQ and HCQ. As expected from the very low bioavailability, pCQ had much lower hepatic accumulation than HCQ with the liver C_{max} for pCQ 58-times lower than the HCQ and ~110-times lower AUC_{0-last} compared to HCQ. It was noteworthy, that pCQ concentrations in the liver declined from the first measured time point and were at all times lower than the liver levels of HCQ ($p \leq 0.001$). These pharmacokinetic differences contributed to the preferential localization of pCQ in the colon as suggested by the calculated colon-to-liver ratios in Fig. 4. The pCQ colon:liver ratio was higher at all measured time points compared to HCQ treatment. Fecal pCQ concentrations were higher than HCQ levels (data not shown). These observations reinforce the applicability of pCQ as a local colonic treatment.

Having established the local colon accumulation of pCQ, it was necessary to analyze pCQ hydrolysis in the GI tract and the extent of release of free HCQ. The content of polymer-bound HCQ and the extent of pCQ hydrolysis have been analyzed using the two different

sample preparation methods described above. As shown in Fig. 5, a clear majority of the HCQ was polymer-bound until at least 8 h post-administration. The released (i.e., free) HCQ levels in the colon decreased, whereas the polymer-bound HCQ levels increased over time. While the released HCQ concentrations were highest in the colon at 1.5 h, the polymer-bound HCQ achieved maximum concentrations at 8 h. Calculating the hydrolyzed fraction at 8 h, only 1.2 % of free HCQ was present in the colon tissue. This indicated that the hydrolyzed HCQ was mostly systemically absorbed and not retained in the epithelium, while the polymer-bound HCQ had a higher transit time to localize in the colon before clearance at 24 h. Estimate of the colon AUC_0-last showed about 37-fold difference between the polymer-bound HCQ and HCQ hydrolyzed from pCQ, suggesting that most of the therapeutic effects described below resulted from the activity of pCQ and not released HCQ. This result proved that pCQ was not degraded to any significant extent and retained its macromolecular character during the GI transit.

3.2.3 HCQ and pCQ metabolism—To address tissue accumulation and subsequent metabolism of HCQ and pCQ, the concentrations of HCQ metabolites in colon and liver were measured at serial time points following oral administration. HCQ is metabolized in the liver by dealkylation into three major metabolites (Fig. 1): desethylchloroquine (DCQ), bisdesethylchloroquine (BDCQ) and desethylhydroxychloroquine (DHCQ) [48]. It has been previously shown that DCQ has similar antimalarial activity as HCQ. All the N-dealkylated metabolites have been implicated in heart failure and retinopathy, with BDCQ being more cardiotoxic than HCQ [49]. Importantly for chronic use in IBD, HCQ and its metabolites have extremely long biological half-lives and thus their monitoring is important.

As expected, pCQ significantly decreased the extent and rate of HCQ metabolism due to the covalent bond formed between the polymer and the hydroxyl in HCQ ($p \leq 0.001$). The metabolite concentration results in liver and colon are shown in Fig. 6. In the liver (Fig. 6a), which is the main organ for HCQ metabolism, both DCQ and BDCQ concentrations were 10–100-fold higher in the HCQ-treated group as compared to the pCQ group. Both DCQ and BDCQ liver concentrations peaked at 8 h. DHCQ liver levels were undetectable in the pCQ group.

Data in Fig. 6b suggest that HCQ metabolism occurs in the colon. In agreement with the liver metabolism findings, metabolite concentrations in the colon were about 10–100-fold lower in the pCQ group than in the HCQ group. Calculating the percent of metabolites in the colon at C_{max} (8 h), it was observed that pCQ was metabolized to a lower extent than HCQ. While the major metabolite DCQ accounted for 16.5 % in the HCQ group, only 4% of pCQ was metabolized to DCQ in the colon. BDCQ (4 % of HCQ vs. 0.4 % of pCQ) and DHCQ (8 % of HCQ vs. 1 % of pCQ) showed similar differences. Subsequently, it was necessary to verify whether the colon metabolism of pCQ resulted in higher than anticipated blood level of metabolites. Analysis of blood metabolite concentrations revealed that most metabolites were either undetectable or significantly lower in the pCQ group as a result of the very low bioavailability (data not shown). This finding, coupled with the observation of elevated fecal pCQ concentrations, further supports pCQ localization in the colon as opposed to systemic absorption. The covalent conjugation of HCQ in pCQ not only reduced its oral absorption due to its macromolecular nature, but it also decreased accessibility to metabolic enzymes,

thus preventing generation of toxic HCQ metabolites. Such a low systemic exposure to HCQ and its metabolites may result in reduction of adverse systemic side effects commonly observed with HCQ.

3.3 Therapeutic efficacy

The local colon accumulation, limited systemic exposure, and low liver distribution of pCQ provided strong rationale for the testing of its anti-inflammatory activity in colitis. Consequently, a therapeutic efficacy study was conducted to assess whether restricting the distribution of pCQ to the GI tract preserves the activity of HCQ. The mice with colitis were treated every other day with oral gavage of pCQ and HCQ. Histological changes in the colon were examined following animal sacrifice on day 14. As shown in Fig. 7, untreated animals showed superficial epithelial damage, marked reduction in the goblet cell population, mucin depletion, inflammatory cell infiltration and crypt hyperplasia [32]. Treatment with both, pCQ and HCQ, reduced the colon inflammation and eased the epithelial injury (Fig. 7a). Statistically significant reduction of the histological damage score was observed in animals treated with pCQ ($p \leq 0.05$) (Fig. 7c). Both treatments significantly reduced the colon crypt length when compared with the untreated group ($p \leq 0.01$ (HCQ), $p \leq 0.001$ (pCQ)) (Fig. 7b). These findings support previous reports showing the efficacy of CQ in DSS-induced model of colitis and human patients [28, 50, 51]. Oral administration of HCQ is associated with GI side effects, including nausea, vomiting, and diarrhea. In this study, we observed no worsening of diarrhea in the animals treated with either HCQ or pCQ, suggesting relative safety of the formulations at the selected doses and administration frequency. More studies are needed to fully assess potential GI side effects of pCQ.

To assess the immunohistochemical changes that occur during inflammation, we studied the effect of pCQ treatment on the expression of two markers (CD68, CC3) that are commonly measured in reported *in vivo* IBD studies. CD68 is a transmembrane glycoprotein specifically expressed by monocytes and macrophages. CD68 plays an important role in macrophage homing to tissues and is used to study macrophage infiltration in the inflamed colon. The elevated infiltration of $CD68^+$ macrophages observed in the colons of untreated mice with colitis was in agreement with reported patient data [52]. Treatment with pCQ and HCQ showed statistically significant reduction in the macrophage infiltration ($p \leq 0.001$), with pCQ outperforming HCQ ($p \leq 0.01$) (Fig. 8b). $CD68^+$ macrophages have different roles in UC and CD, but they massively infiltrate throughout the inflamed colon [53] and targeting CD68 to reduce macrophage infiltration is a potential therapeutic strategy in IBD [54]. Based on prior work which showed a broad ability of pCQ to inhibit migration and invasion of cells, reduction of macrophage infiltration could be a possible mechanism by which pCQ is exerting its anti-inflammatory activity. Subsequently, apoptosis was evaluated as a marker for epithelial cell injury. The CC3 immunostaining was used to assess the apoptotic cells in the colon epithelium. pCQ treatment showed statistically significant reduction in the number of apoptotic epithelial cells when compared with the untreated group ($p \leq 0.001$) (Fig. 9). This observation combined with the decrease in the crypt length demonstrates the amelioration of epithelial cell injury by pCQ.

Overall, we found that pCQ had significantly enhanced anti-inflammatory efficacy relative to HCQ at dose-equivalent amounts despite similar colon exposure of both treatments. Although detailed mechanistic understanding is not available at the moment, the observed improvement is likely due to the combination of longer colon residence time of pCQ relative to HCQ and potentially also due to the multivalency effect of pCQ which may improve interactions with the therapeutic target.

3.4 Mechanism of action

Following histological evaluation, possible mechanisms for the anti-inflammatory activity of pCQ were explored. Upregulation of pro-inflammatory cytokines is a hallmark of IBD and lowering local levels of cytokines has been shown to reduce colon inflammation. To investigate how pCQ treatment changes the cytokine expression profile, mRNA levels of selected pro-inflammatory cytokines in the colons after oral administration of seven doses of pCQ over 14 days were measured. Although inhibition of TNFα is a well-established approach in the treatment of IBD and TNFα mRNA expression was 5-times higher in the untreated group, no significant reduction in the colon TNFα mRNA expression was observed after treatment with pCQ (Fig. 10a). Subsequently, expression levels of IL-6, IL-1β and IL-2 in the colon were assessed. Initial animal model suitability studies indicated that IL-6 was highly upregulated in the *C. rodentium* model. Here, statistically significant reduction of IL-6 expression by both pCQ and HCQ was observed ($p \leq 0.01$, $p \leq 0.05$, respectively) (Fig. 10b). pCQ and HCQ treatments had a similar effect on the expression of IL-1β (Fig. 10c). The finding that despite the overall improvement in the colon histology (Fig. 7), only IL-6 but not TNFα expression was positively affected by the pCQ treatment, point to the need for combination therapeutic approach with TNFα inhibitors.

In contrast to IL-6 and IL1β, both treatments resulted in upregulated IL-2 expression (Fig. 10d). Statistically significant difference was observed between IL-2 levels in untreated control and pCQ group ($p \leq 0.05$). IL-2 knockout mice are an often-used animal model of IBD and there has been a reported clinical trial which investigated subcutaneously administered IL-2 as a way of enhancing regulatory T cells in IBD patients to reduce inflammation [55]. Based on these findings, upregulation of IL-2 may represent an interesting direction in the mechanistic studies of pCQ anti-inflammatory activity.

To further elucidate the mechanism of pCQ action, the expression of STAT3, which is a downstream target of IL-6 with a known importance in the development of IBD was measured [56, 57]. Upon activation, STAT3 translocates from the cell cytoplasm to the nucleus and regulates gene transcription related to proliferation, migration, apoptosis, and survival. STAT3 activation plays an important role in several autoimmune diseases including IBD [58]. It was interesting that despite similar overall expression of STAT3 between the treatment groups, there was a significant increase in the nuclear STAT3 expression in the *C. rodentium* infected mice. The nuclear STAT3 localization was reversed back towards the cytoplasmic localization after treatment with pCQ and HCQ. Quantitative analysis demonstrated that the inhibitory effect of pCQ on STAT3 activation was superior to the effect of HCQ (Fig. 11a and 11b). Of note, IL-6 and STAT3 have been targets of multiple mechanistic as well as clinical and preclinical studies, and have also been implicated in

promoting colon cancer [57]. The IL-6 and STAT3 pathways promote immune response by increasing the $CD4^+$ T-cell migration into the inflamed colon, which consequently increases the migration of other immune cells to the inflamed areas [59]. Accumulated evidence suggests that activation of IL-6 and STAT3 is an important inflammatory event in the development of IBD. Hence, inhibiting IL-6 and STAT3 signaling pathways represents a possible mechanism of action for the observed anti-inflammatory activity of pCQ [60]. Overall, observations from the study pointed out that the therapeutic activity of pCQ appeared to be an effect of restoring the colonic immune imbalance that occurs in IBD.

4. CONCLUSION

This is the first report of the local anti-inflammatory effect of non-degradable and non-absorbable polymeric form of HCQ. The study has demonstrated promising therapeutic efficacy of pCQ using the murine model of *C. rodentium* colitis. Despite comparable colon accumulation and reduction in inflammation as HCQ, pCQ showed significant reduction in systemic absorption in mice subjected to colitis. When combined with the already established lower cytotoxicity of pCQ, this finding is an important step in improving safety profile of HCQ while maintaining its anti-inflammatory activity. Improvement of pCQ accumulation and uptake in the inflamed colon is likely to further enhance the anti-inflammatory effect. Formulating pCQ as particles is one of the potential strategies that can be explored to achieve enhanced uptake. Several putative mechanisms of action for pCQ as an anti-inflammatory agent were identified. Imbalance of the immune system plays a major role in IBD and the investigation suggests that pCQ may restore the homeostasis between the pro-inflammatory and anti-inflammatory aspects of the immune system in the colon. Future studies will seek to investigate the exact mechanism of local anti-inflammatory effect of pCQ including the potential binding ability to TLR-9. Additional focus of the future studies will be on testing pCQ in other models of IBD to validate the broad applicability of the approach. As recommended during review of this manuscript, the taste of the developed pCQ will be evaluated and compared with the parent drug to assess if pCQ provides better patient acceptability.

Acknowledgements.

This work was supported by startup funds from the University of Nebraska Medical Center (DO), National Institutes of Health (EB020308 to DO and DK088902 to ABS), VA-merit award BX002761 to ABS, and by the Fred and Pamela Buffett Cancer Center Support Grant from the National Cancer Institute under the award number P30 CA036727 to DM.

REFERENCES

[1]. Ponder A, Long MD, A clinical review of recent findings in the epidemiology of inflammatory bowel disease, Clin. Epidemiol, 5 (2013) 237–247. [PubMed: 23922506]

[2]. Vermeire S, Ferrante M, Rutgeerts P, Recent advances: personalised use of current Crohn's disease therapeutic options, Gut, 62 (2013) 1511–1515. [PubMed: 24037876]

[3]. Talley NJ, Abreu MT, Achkar J-P, Bernstein CN, Dubinsky MC, Hanauer SB, Kane SV, Sandborn WJ, Ullman TA, Moayyedi P, An Evidence-Based Systematic Review on Medical Therapies for Inflammatory Bowel Disease, Am. J. Gastroenterol, 106 (2011) S2–S25. [PubMed: 21472012]

[4]. Abraham C, Cho JH, Inflammatory Bowel Disease, N. Engl. J. Med, 361 (2009) 2066–2078. [PubMed: 19923578]

[5]. Nielsen OH, Coskun M, Steenholdt C, Rogler G, The role and advances of immunomodulator therapy for inflammatory bowel disease, Expert Rev. Gastroenterol. Hepatol, 9 (2015) 177–189. [PubMed: 25101818]

[6]. Feagan BG, MacDonald JK, Oral 5-aminosalicylic acid for induction of remission in ulcerative colitis, Cochrane Database Syst. Rev, 10 (2012).

[7]. Mahadevan U, Medical Treatment of Ulcerative Colitis, Clin. Colon Rectal Surg, 17 (2004) 7–19. [PubMed: 20011280]

[8]. Rutgeerts PJ, The limitations of corticosteroid therapy in Crohn's disease, Aliment. Pharmacol. Ther, 15 (2001) 1515–1525. [PubMed: 11563990]

[9]. Keane J, Gershon S, Wise RP, Mirabile-Levens E, Kasznica J, Schwieterman WD, Siegel JN, Braun MM, Tuberculosis Associated with Infliximab, a Tumor Necrosis Factor α– Neutralizing Agent, N. Engl. J. Med, 345 (2001) 1098–1104. [PubMed: 11596589]

[10]. Friend DR, New oral delivery systems for treatment of inflammatory bowel disease, Adv. Drug Deliv. Rev, 57 (2005) 247–265. [PubMed: 15555741]

[11]. Hua S, Marks E, Schneider JJ, Keely S, Advances in oral nano-delivery systems for colon targeted drug delivery in inflammatory bowel disease: Selective targeting to diseased versus healthy tissue, Nanomedicine., 11 (2015) 1117–1132. [PubMed: 25784453]

[12]. Hu Z, Mawatari S, Shibata N, Takada K, Yoshikawa H, Arakawa A, Yosida Y, Application of a Biomagnetic Measurement System (BMS) to the Evaluation of Gastrointestinal Transit of Intestinal Pressure-Controlled Colon Delivery Capsules (PCDCs) in Human Subjects, Pharm. Res, 17 (2000) 160–167. [PubMed: 10751030]

[13]. Coupe AJ, Davis SS, Wilding IR, Variation in Gastrointestinal Transit of Pharmaceutical Dosage Forms in Healthy Subjects, Pharm. Res, 8 (1991) 360–364. [PubMed: 2052525]

[14]. Fallingborg J, Christensen LA, Jacobsen BA, Rasmussen SN, Very low intraluminal colonic pH in patients with active ulcerative colitis, Dig. Dis. Sci, 38 (1993) 1989–1993. [PubMed: 8223071]

[15]. Nugent SG, Kumar D, Rampton DS, Evans DF, Intestinal luminal pH in inflammatory bowel disease: possible determinants and implications for therapy with aminosalicylates and other drugs, Gut, 48 (2001) 571–577. [PubMed: 11247905]

[16]. Laukoetter MG NP, Nusrat, Role of the intestinal barrier in inflammatory bowel disease, World J. Gastroenterol, 14 (2008) 401–407. [PubMed: 18200662]

[17]. Malayandi R, Kondamudi PK, Ruby PK, Aggarwal D, Biopharmaceutical considerations and characterizations in development of colon targeted dosage forms for inflammatory bowel disease, Drug Deliv. Transl. Res, 4 (2014) 187–202. [PubMed: 25786732]

[18]. Collnot E-M, Ali H, Lehr C-M, Nano- and microparticulate drug carriers for targeting of the inflamed intestinal mucosa, J. Control. Release, 161 (2012) 235–246. [PubMed: 22306429]

[19]. Tirosh B, Khatib N, Barenholz Y, Nissan A, Rubinstein A, Transferrin as a Luminal Target for Negatively Charged Liposomes in the Inflamed Colonic Mucosa, Mol. Pharm, 6 (2009) 1083–1091. [PubMed: 19603812]

[20]. Xiao B, Laroui H, Ayyadurai S, Viennois E, Charania MA, Zhang Y, Merlin D, Mannosylated bioreducible nanoparticle-mediated macrophage-specific TNF-α RNA interference for IBD therapy, Biomaterials, 34 (2013) 7471–7482. [PubMed: 23820013]

[21]. Xiao B, Laroui H, Viennois E, Ayyadurai S, Charania MA, Zhang Y, Zhang Z, Baker MT, Zhang B, Gewirtz AT, Merlin D, Nanoparticles With Surface Antibody Against CD98 and Carrying CD98 Small Interfering RNA Reduce Colitis in Mice, Gastroenterology, 146 (2014) 1289–1300. [PubMed: 24503126]

[22]. Sanchis J, Canal F, Lucas R, Vicent M, Polymer–drug conjugates for novel molecular targets, Nanomedicine., 5 (2010) 915–935. [PubMed: 20735226]

[23]. Varshosaz J, Emami J, Tavakoli N, Fassihi A, Minaiyan M, Ahmadi F, Dorkoosh F, Synthesis and evaluation of dextran–budesonide conjugates as colon specific prodrugs for treatment of ulcerative colitis, Int. J. Pharm, 365 (2009) 69–76. [PubMed: 18804521]

[24]. Keely S, Ryan SM, Haddleton DM, Limer A, Mantovani G, Murphy EP, Colgan SP, Brayden DJ, Dexamethasone–pDMAEMA polymeric conjugates reduce inflammatory biomarkers in human intestinal epithelial monolayers, J. Control. Release, 135 (2009) 35–43. [PubMed: 19110018]

[25]. Freedman A, Steinberg VL, Chloroquine in Rheumatoid Arthritis: A Double Blindfold Trial of Treatment for One Year, Ann. Rheum. Dis, 19 (1960) 243–250. [PubMed: 13701598]

[26]. Oh S, Shin JH, Jang EJ, Won HY, Kim HK, Jeong M-G, Kim KS, Hwang ES, Anti-inflammatory activity of chloroquine and amodiaquine through p21-mediated suppression of T cell proliferation and Th1 cell differentiation, Biochem. biophys. res. commun, 474 (2016) 345–350.

[27]. Fox RI, Mechanism of action of hydroxychloroquine as an antirheumatic drug, Semin. Arthritis Rheum, 23 (1993) 82–91. [PubMed: 8278823]

[28]. Nagar J, Ranade S, Kamath V, Singh S, Karunanithi P, Subramani S, Venkatesh K, Srivastava R, Dudhgaonkar S, Vikramadithyan RK, Therapeutic potential of chloroquine in a murine model of inflammatory bowel disease, Int. Immunopharmacol, 21 (2014) 328–335. [PubMed: 24859061]

[29]. Latasiewicz M, Gourier H, Yusuf IH, Luqmani R, Sharma SM, Downes SM, Hydroxychloroquine retinopathy: an emerging problem, Eye., 31 (2017) 972–976. [PubMed: 28186509]

[30]. Yusuf IH, Sharma S, Luqmani R, Downes SM, Hydroxychloroquine retinopathy, Eye., 31 (2017) 828–845. [PubMed: 28282061]

[31]. Yu F, Li J, Xie Y, Sleightholm RL, Oupický D, Polymeric chloroquine as an inhibitor of cancer cell migration and experimental lung metastasis, J. Control. Release, 244 (2016) 347–356. [PubMed: 27473763]

[32]. Koroleva EP, Halperin S, Gubernatorova EO, Macho-Fernandez E, Spencer CM, Tumanov AV, Citrobacter rodentium-induced colitis: A robust model to study mucosal immune responses in the gut, J. Immunol. Methods, 421 (2015) 61–72. [PubMed: 25702536]

[33]. Chhonker YS, Sleightholm RL, Li J, Oupický D, Murry DJ, Simultaneous quantitation of hydroxychloroquine and its metabolites in mouse blood and tissues using LC–ESI–MS/MS: An application for pharmacokinetic studies, J. Chromatogr. B Analyt. Technol. Biomed. Life Sci, 1072 (2018) 320–327.

[34]. Wu X, Vallance BA, Boyer L, Bergstrom KSB, Walker J, Madsen K, Kusky JR, Buchan AM, Jacobson K, Saccharomyces boulardii ameliorates Citrobacter rodentium induced colitis through actions on bacterial virulence factors, Am. J. Physiol. Gastrointest. Liver Physiol, 294 (2008) G295–306. [PubMed: 18032474]

[35]. Mizoguchi A, Animal Models of Inflammatory Bowel Disease, Prog. Mol. Biol. Transl. Sci, 105 (2012) 263–320. [PubMed: 22137435]

[36]. Borenshtein D, McBee M, B Schauer D, Utility of the Citrobacter rodentium infection model in laboratory mice, Curr. Opin. Gastroenterol., 24 (2008) 32–37.

[37]. Guan G, Wang H, Chen S, Liu G, Xiong X, Tan B, Duraipandiyan V, Al-Dhabi NA, Fang J, Dietary Chitosan Supplementation Increases Microbial Diversity and Attenuates the Severity of Citrobacter rodentium Infection in Mice, Mediators Inflamm., 2016 (2016) 9236196. [PubMed: 27761062]

[38]. Higgins LM, Frankel G, Connerton I, Gonçalves NS, Dougan G, MacDonald TT, Role of Bacterial Intimin in Colonic Hyperplasia and Inflammation, Science, 285 (1999) 588–591. [PubMed: 10417389]

[39]. Higgins LM, Frankel G, Douce G, Dougan G, MacDonald TT, Citrobacter rodentium Infection in Mice Elicits a Mucosal Th1 Cytokine Response and Lesions Similar to Those in Murine Inflammatory Bowel Disease, Infect. Immun, 67 (1999) 3031–3039. [PubMed: 10338516]

[40]. Jain U, Cao Q, Thomas NA, Woodruff TM, Schwaeble WJ, Stover CM, Stadnyk AW, Properdin Provides Protection from Citrobacter rodentium–Induced Intestinal Inflammation in a C5a/IL-6–Dependent Manner, J. Immunol, 194 (2015) 3414. [PubMed: 25725105]

[41]. Johnson-Henry KC, Nadjafi M, Avitzur Y, Mitchell DJ, Ngan B-Y, Galindo-Mata E, Jones NL, Sherman PM, Amelioration of the Effects of Citrobacter rodentium Infection in Mice by Pretreatment with Probiotics, J. Infect. Dis, 191 (2005) 2106–2117. [PubMed: 15897997]

[42]. Luperchio SA, Newman JV, Dangler CA, Schrenzel MD, Brenner DJ, Steigerwalt AG, Schauer DB, Citrobacter rodentium, the Causative Agent of Transmissible Murine Colonic Hyperplasia, Exhibits Clonality: Synonymy of C. rodentium and Mouse-Pathogenic Escherichia coli, J. Clin. Microbiol, 38 (2000) 4343–4350. [PubMed: 11101562]

[43]. Wiles S, Pickard KM, Peng K, MacDonald TT, Frankel G, In Vivo Bioluminescence Imaging of the Murine Pathogen Citrobacter rodentium, Infect. Immun, 74 (2006) 5391–5396. [PubMed: 16926434]

[44]. Solomon L, Mansor S, Mallon P, Donnelly E, Hoper M, Loughrey M, Kirk S, Gardiner K, The dextran sulphate sodium (DSS) model of colitis: an overview, Comp. Clin. Path, 19 (2010) 235–239.

[45]. Araki Y, Bamba T, Mukaisho K, Kanauchi O, Ban H, Bamba S, Andoh A, Fujiyama Y, Hattori T, Sugihara H, Dextran sulfate sodium administered orally is depolymerized in the stomach and induces cell cycle arrest plus apoptosis in the colon in early mouse colitis, Oncol. Rep, 28 (2012) 1957–1605.

[46]. Kerr TA, Ciorba MA, Matsumoto H, Davis VRT, Luo J, Kennedy S, Xie Y, Shaker A, Dieckgraefe BK, Davidson NO, Dextran Sodium Sulfate Inhibition of Real-Time PCR Amplification: A Poly-A Purification Solution, Inflamm. Bowel Dis., 18 (2012) 344–348.

[47]. Smith AD, Botero S, Shea-Donohue T, Urban JF, The Pathogenicity of an Enteric Citrobacter rodentium Infection Is Enhanced by Deficiencies in the Antioxidants Selenium and Vitamin E, Infect. Immun, 79 (2011) 1471–1478. [PubMed: 21245271]

[48]. Browning DJ, Pharmacology of Chloroquine and Hydroxychloroquine, in: Browning DJ (Ed.) Hydroxychloroquine and Chloroquine Retinopathy, Springer New York, New York, NY, 2014, pp. 35–63.

[49]. Ducharme J, Farinotti R, Clinical Pharmacokinetics and Metabolism of Chloroquine, Clin. Pharmacokinet, 31 (1996) 257–274. [PubMed: 8896943]

[50]. Goenka M, Kocchar R, Tandia B, Mehta S, Chloroquine for mild to moderately active ulcerative colitis: comparison with sulfasalazine, Am. J. Gastroenterol, 91 (1996) 917–921. [PubMed: 8633581]

[51]. Mayer L, Present D, Effect of hydroxychloroquine in the treatment of active ulcerative colitis: results of the open label phase of controlled study, Gastroenterology, 100 (1991) A230.

[52]. Rugtveit J, Brandtzaeg P, Halstensen TS, Fausa O, Scott H, Increased macrophage subset in inflammatory bowel disease: apparent recruitment from peripheral blood monocytes, Gut, 35 (1994) 669–674. [PubMed: 8200563]

[53]. Kühl AA, Erben U, Kredel LI, Siegmund B, Diversity of Intestinal Macrophages in Inflammatory Bowel Diseases, Front. Immunol, 6 (2015) 613. [PubMed: 26697009]

[54]. Chistiakov DA, Killingsworth MC, Myasoedova VA, Orekhov AN, Bobryshev YV, CD68/macrosialin: not just a histochemical marker, Lab. Invest, 97 (2017) 4–13.

[55]. Goettel J, Kotlarz D, Illig D, Canavan J, Allegretti J, Hamilton M, Kelly R, Griffith A, Carellas M, Nelina A, Bousvaros A, Korzenik J, Snapper S, O-011 Low-dose IL-2 Administration Expands Human Regulatory T Cells in Patients with UC and Humanized Mice and Protects Against Experimental Colitis, Inflamm. Bowel Dis, 23 (2017) S4.

[56]. Bernardo D, Vallejo-Díez S, Mann ER, Al-Hassi HO, Martínez-Abad B, Montalvillo E, Tee CT, Murugananthan AU, Núñez H, Peake STC, Hart AL, Fernández-Salazar L, Garrote JA, Arranz E, Knight SC, IL-6 promotes immune responses in human ulcerative colitis and induces a skin-homing phenotype in the dendritic cells and T cells they stimulate, Eur. J. Immunol, 42 (2012) 1337–1353. [PubMed: 22539302]

[57]. Noguchi D, Wakita D, Tajima M, Ashino S, Iwakura Y, Zhang Y, Chamoto K, Kitamura H, Nishimura T, Blocking of IL-6 signaling pathway prevents CD4+ T cell-mediated colitis in a Th17-independent manner, Int. Immunol, 19 (2007) 1431–1440. [PubMed: 17981790]

[58]. Sugimoto K, Role of STAT3 in inflammatory bowel disease, World J. Gastroenterol,14 (2008) 5110–5114. [PubMed: 18777586]

[59]. Yamamoto M, Yoshizaki K, Kishimoto T, Ito H, IL-6 Is Required for the Development of Th1 Cell-Mediated Murine Colitis, J. Immunol, 164 (2000) 4878–4882. [PubMed: 10779797]

[60]. Mariangela A, Manol J, Gionata F, Stefan S, Silvio D, Anti-IL-6 Treatment for Inflammatory Bowel Diseases: Next Cytokine, Next Target, Curr. Drug Targets, 14 (2013) 1508–1521. [PubMed: 24102406]

Statement of Significance

Inflammatory bowel disease is a chronic localized inflammation of the gastrointestinal tract with no effective cure. Despite being widely researched in anti-inflammatory studies, chloroquine has limited application in inflammatory bowel disease due to its limitations in chronic administration setting due to high systemic absorption related side effects. Various studies have shown that the local gastrointestinal accumulation can be improved by using polymeric drugs. The reported study provides quantitative data relating to the applicability of non-degradable polymeric chloroquine as a local therapy of inflammatory bowel disease. The main significance of this study is in the design of novel macromolecular agents for oral, locally acting anti-inflammatory therapies.

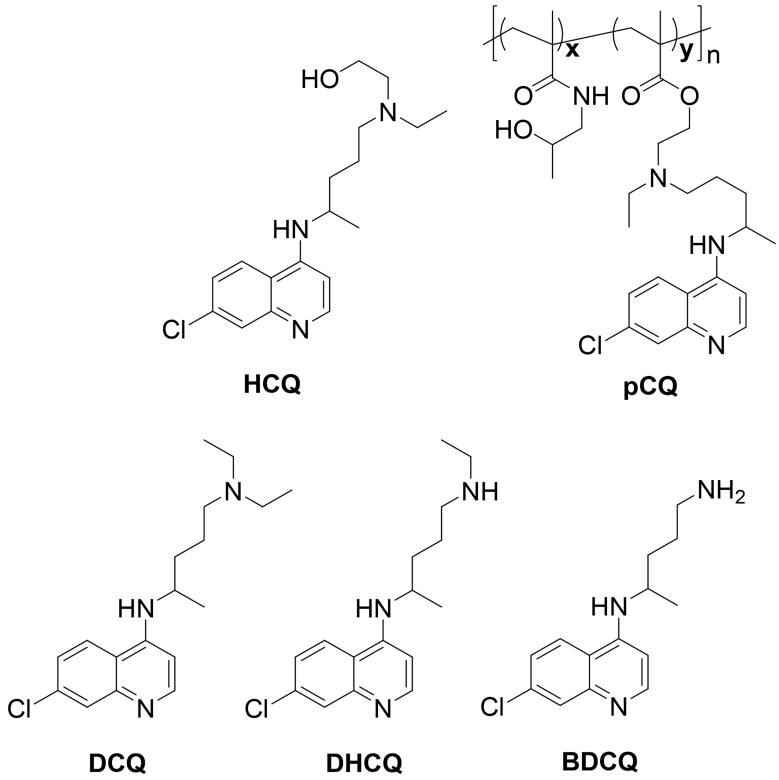

Figure 1.
Chemical structures of HCQ, pCQ, and main HCQ metabolites.

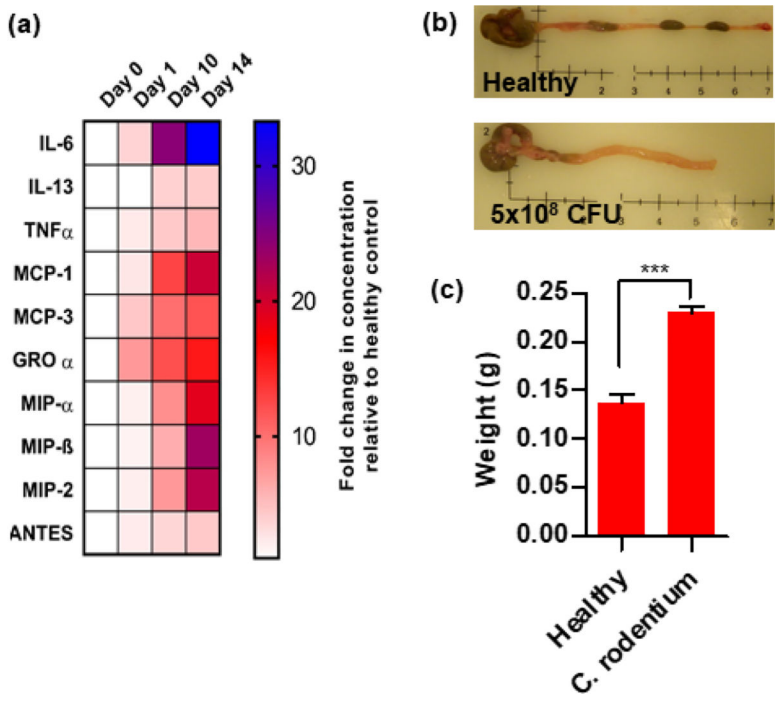

Figure 2. Analysis of *C. rodentium* colitis.

Mice were gavaged with 5×10^8 CFU of C. rodentium and sacrificed on day 1, 10, and 14. (a) Cytokine levels in the colon homogenates were analyzed using Luminex ProcartaPlex panel. Data are represented as mean fold change vs. healthy animals. (b) Representative images of colon (Day 14). (c) Colon weight (Day 14).

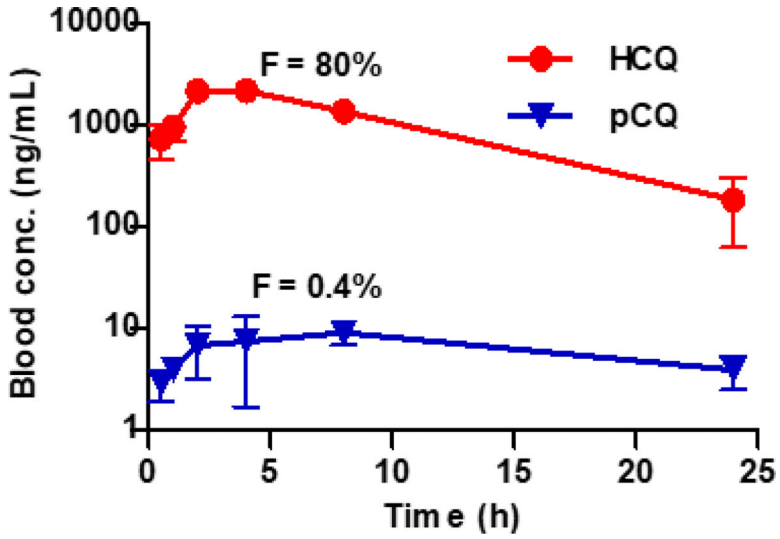

Figure 3. Blood concentration vs. time profile.

Mice subjected to the *C. rodentium* colitis were orally administered with HCQ or pCQ (30 mg/kg HCQ equivalent). Results are shown as HCQ blood concentration ± SD (n=3). Data shown represent the total (polymer-bound + free) HCQ blood concentration in the pCQ treatment.

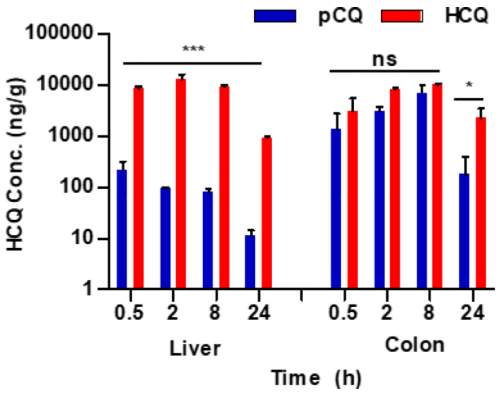

	Colon-to-Liver ratio	
Time (h)	pCQ	HCQ
2	33	0.7
8	89	1.1
24	16	2.1

Figure 4. Liver and colon distribution of pCQ in colitis mice.

Animals treated with a single oral dose of pCQ and HCQ (30 mg/kg CQ equivalent) were sacrificed at pre-determined time points and total HCQ levels measured in liver and colon. Results are shown as concentration of HCQ in the tissues ± SD (n=3). pCQ data show the total (polymer-bound + free) HCQ blood concentration.

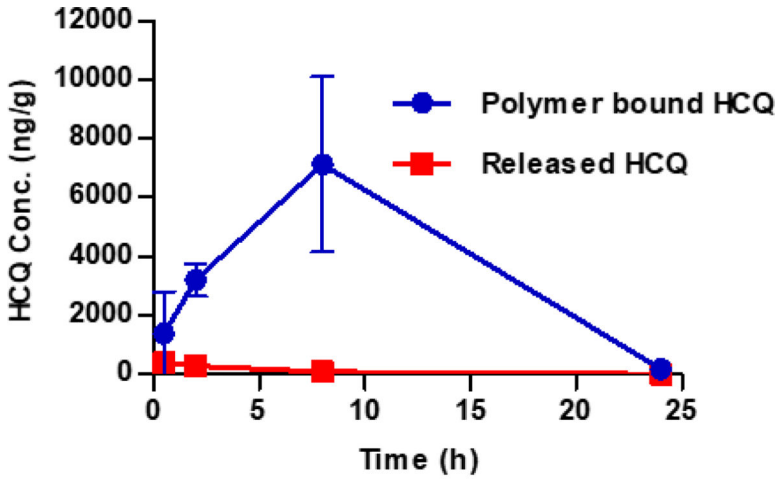

$AUC_{0\text{-last}}$ (h*ng/ml)	
Polymer bound HCQ	93087.8
Released HCQ	2470.5

Figure 5. Hydrolysis of pCQ in the colon.

Concentration of polymer-bound and free HCQ were measured in colons from colitis mice. Results are expressed as HCQ conc. ± SD (n=3).

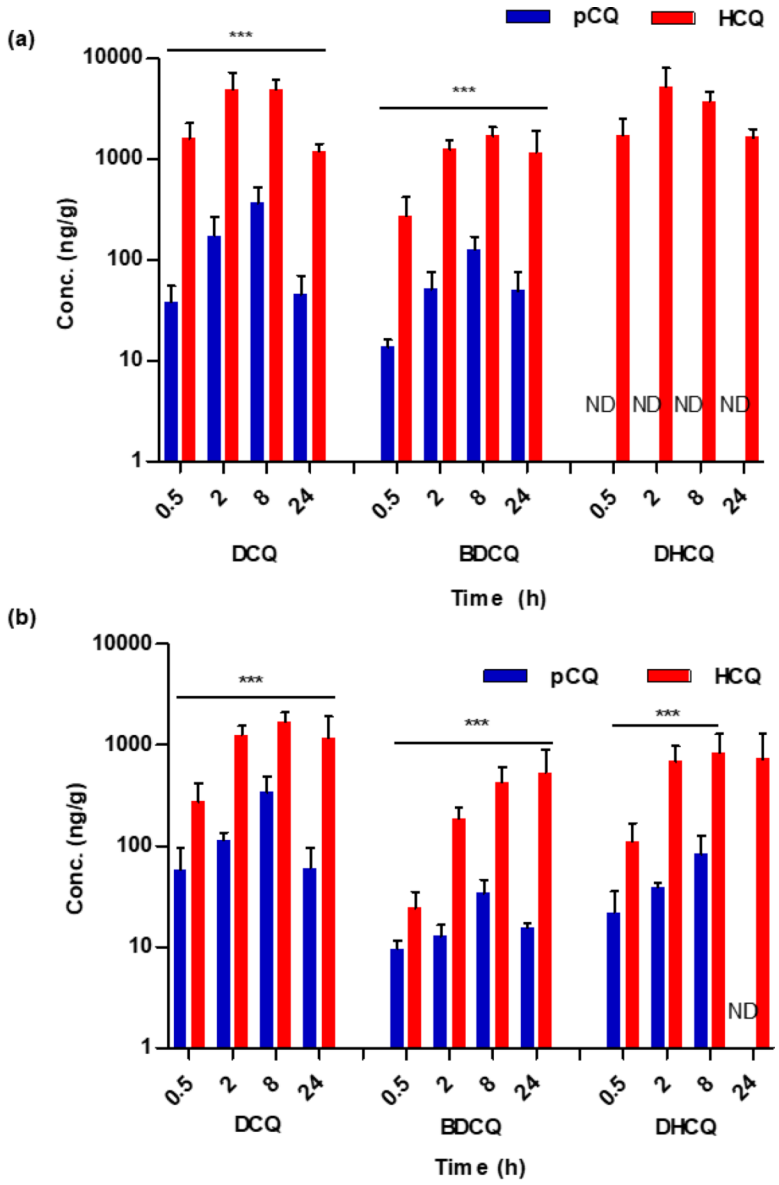

Figure 6. Liver (a) and colon (b) metabolism of pCQ and HCQ.

Tissue homogenates were analyzed for metabolites. Data are represented as mean metabolite concentration in ng/g of tissue ± SD.

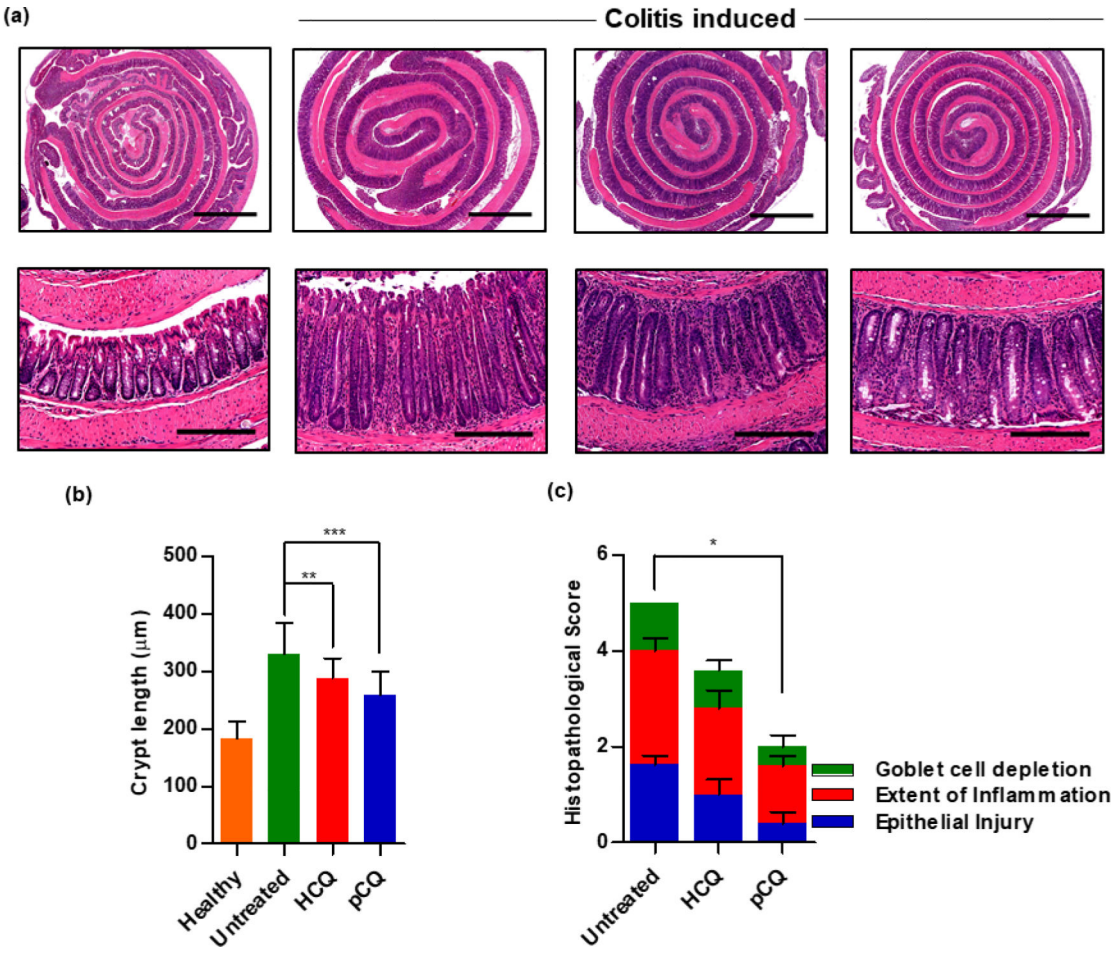

Figure 7. Effect of oral pCQ on colon inflammation.

Mice with *C. rodentium* colitis were orally administered with seven pCQ or HCQ doses (30 mg/kg CQ). (a) Representative images of H&E stained colon (Upper panel: 2x, Lower panel: 20x magnification, Scale bars: 200 μm); (b) colon crypt length; (c) histopathological score. Data are represented as mean ± SD (n=5).

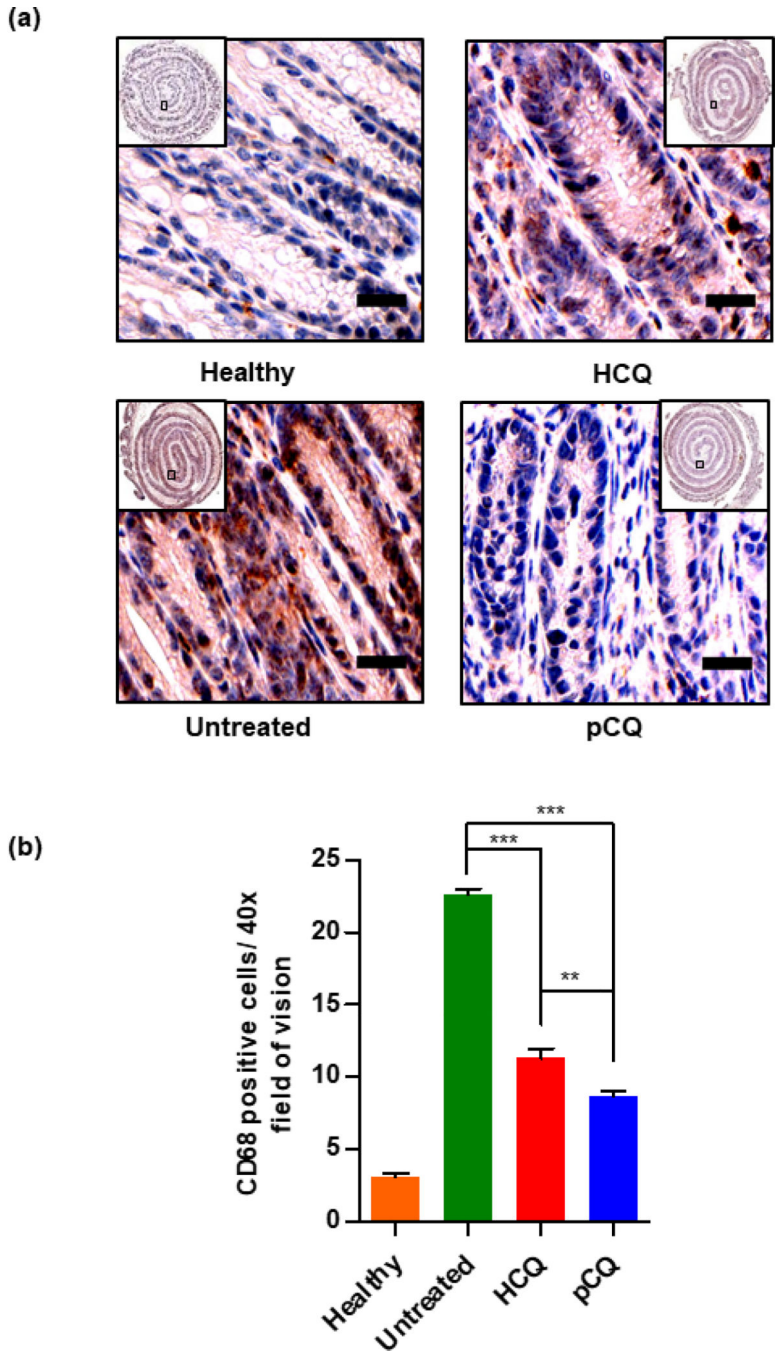

Figure 8. Effect of pCQ on macrophage infiltration in the colon.

(a) Representative images of CD68-stained colon tissue slides (20x magnification, Scale bars: 50 μm); (b) Quantitation of the CD68-positive cells. Data are represented as mean CD68 positive cells per HPF ± SD.

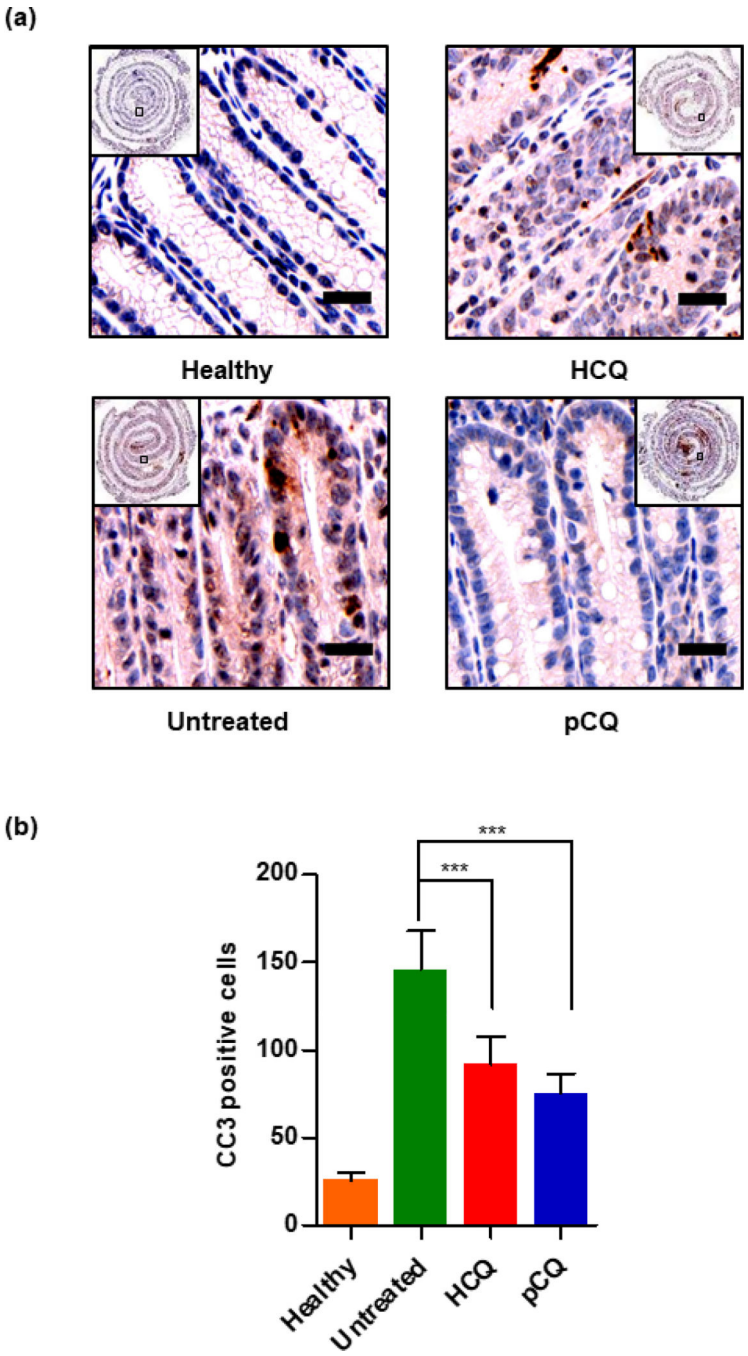

Figure 9. Effect of pCQ on epithelial apoptosis.

(a) Representative images of CC3 stained colon tissue slides (20x magnification, Scale bars: 50 μm); (b) quantitation of CC3-positive cells. Data are represented as mean CC3 positive cells/colon section ± SD. (50 μm, 40x)

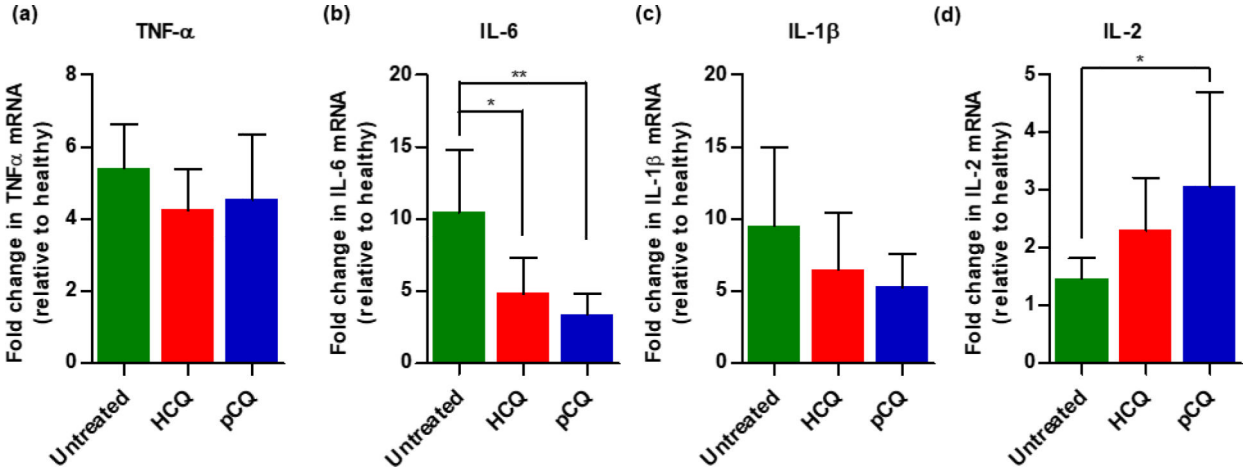

Figure 10. Effect of pCQ on colon cytokine mRNA levels.

Fold change in colon mRNA expression relative to healthy control (a) TNF-α; (b) IL-6; (c) IL-1β; and (d) IL-2. Data are represented as mean ± SD (n=5).

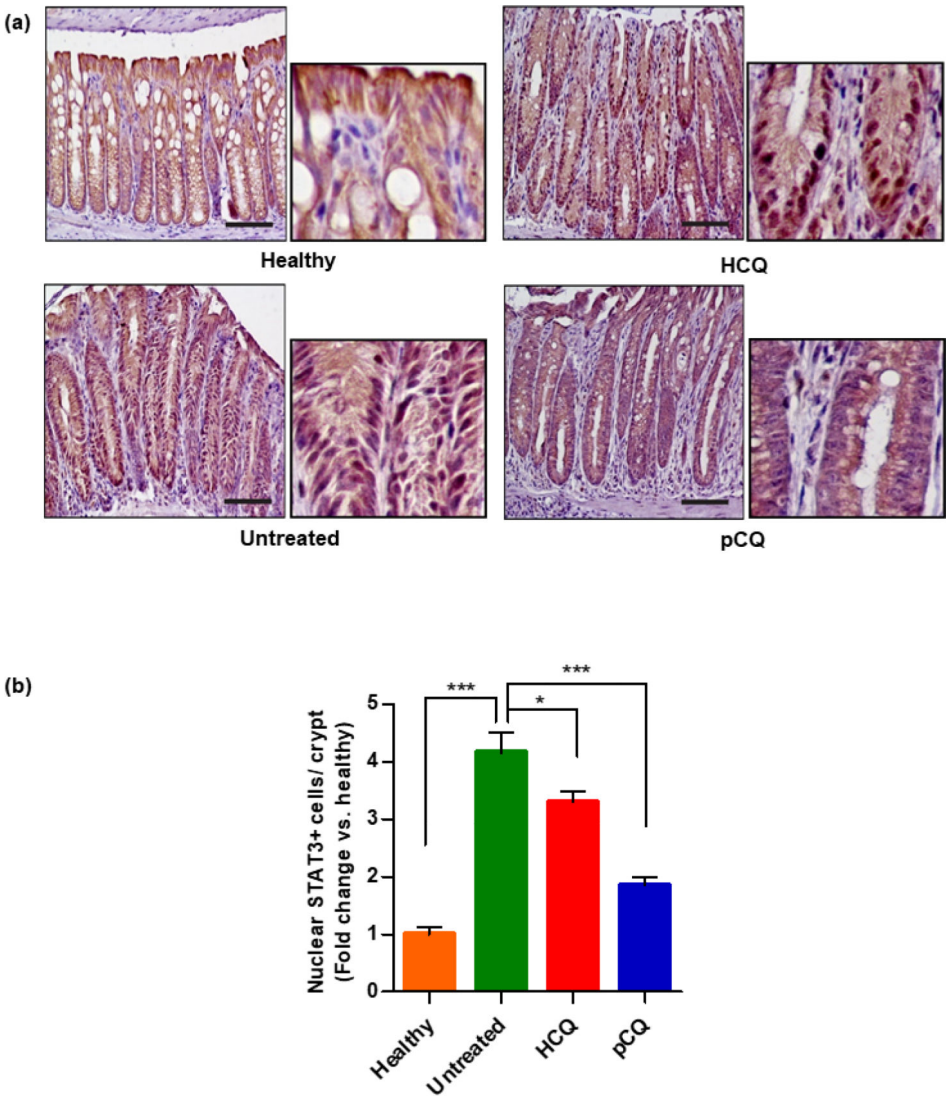

Figure 11. Effect of HCQ and pCQ on STAT3 activation.

(a) Representative images showing nuclear STAT3 localization in the colon. (larger panel: 20x magnification, smaller panel: 40x magnification, scale bars: 100 μm) (b) Respective counting of STAT3 nuclear positive cells per crypt in colon tissue slides.

Table 1.

Primer sequences for RT-PCR

mRNA targets	Primer sequence (5'−3')	
TNF-α	F	CATGAGCACAGAAAGCATGATC
	R	CCTTCTCCAGCTGGAAGACT
IL-6	F	ATGGATGCTACCAACTGGAT
	R	TGAAGGACTCTGGCTTTGTCT
IL-1β	F	CAACCAACAAGTGATATTCTCCATG
	R	GATCCACACTCTCCAGCTGCA
IL-2	F	TGAGCAGGATGGAGAATTACAGG
	R	GTCCAAGTTCATCTTCTAGGCAC

Table 2.

Non-compartmental blood pharmacokinetic analysis in colitis mice

Pharmacokinetic parameter	HCQ	pCQ
C_{max} (ng/mL)	2,343 ± 46	12.2 ± 1.7
$t_{1/2}$ (h)	5.6 ± 1.9	11.7 ± 3.6
t_{max} (h)	3.3 ± 1.2	4.7 ± 3.1
$AUC_{0\text{-}last}$ (h×ng/mL)	26,446 ± 507	161 ± 8
$AUC_{0\text{-}\infty}$ (h×ng/mL)	28,182 ± 1476	231 ± 49
Cl/F (L/h/kg)	1.1 ± 0.1	134 ± 27
MRT (h)	6.8 ± 0.6	9.9 ± 0.7

Table 3.

Liver and colon pharmacokinetic parameters in colitis mice.

Pharmacokinetic parameter	Liver HCQ	pCQ	Colon HCQ	pCQ
C_{max} (ng/mL)	12,807±3703	220.2±102.7	10,304 ± 746	7,121 ± 2,984
t_{max} (h)	2.0±0.0	0.5±0.0	8.0±0.0	8.0±0.0
$AUC_{0\text{-last}}$ (h×ng/mL)	167,944 ± 19,302	1,547 ± 100	166,377 ± 14,873	93,088 ± 34,403
$AUC_{0\text{-}\infty}$ (h×ng/mL)	175,852 ± 18,362	1,659 ± 78	208,917 ± 55,806	94,515 ± 35,363